Closed-Loop Control of the Orbit Evolution of 'Smart Dust' Swarms

Ming Xu [1,2,†] and **Colin R McInnes** [2,‡]

[1] *Beihang University, Beijing 100191, China;* [2] *University of Glasgow, Glasgow G12 8QQ, UK*

I. Introduction

Benefiting from developments in micro-electromechanical systems (MEMS), a new spacecraft architecture termed 'SpaceChip' [1], 'ChipSats' [2] or 'smart dust' [3] swarms has been proposed to distribute sensing nodes in heliocentric orbit to enable massively parallel space science. Due to the low cost of such swarms, smaller and cheaper even than CubeSats, they are seen as disposable sensors that could be used on missions to explore hostile environments, beyond the capability of traditional spacecraft architectures [2]. For a single 'smart dust' device of decreasing length-scale L in heliocentric orbit, its mass and surface area scale as L^3 and L^2 respectively, resulting in an increasing area-to-mass ratio for smaller devices. Such devices are strongly perturbed by solar radiation pressure (SRP). Therefore, the orbit evolution of a swarm of devices can in principle by controlled through modulation of its pitch angle or lightness number [4].

To model the orbit evolution of such a swarm, it is preferable to use partial differential equations (PDE), akin to fluid mechanics dealing with continuum flow, rather than ordinary differential equations (ODEs) traditionally used in astrodynamics. This continuum approach to astrodynamics originates from studies on the evolution of natural dust clouds, debris clouds and the West Ford Needles, a passive swarm of 1.8 cm long wires [5,6]. Gor'Kavyi et al. [7,8] considered the natural evolution of interplanetary dust under Poynting-Roberson drag and planetary resonances by introducing a continuity PDE and then integrating it numerically to find quasi-stationary states for natural dust flows. Considering the natural evolution of Earth-orbiting nanosatellite constellations under air drag, on-orbit failures and the deposition of new satellites into the constellation, McInnes [9] derived a set of PDEs with the same form as Gor'Kavyi et al [7]. He then obtained closed-form analytic solutions to these PDEs which provide insights into the global dynamics and long-term evolution of large constellations of nanosatellites. Asymptotic steady-state distributions of nanosatellites constellations were also found and an estimate of the required deposition rate of new nanosatellites to maintain a constellation provided. This PDE approach with closed-form solutions was then extended to investigate wave-like

† Associate professor, School of Astronautics; currently China Scholarship Council Research Fellow, School of Engineering, University of Glasgow; xuming@buaa.edu.cn.

‡ James Watt Chair, Professor of Engineering Science, School of Engineering, colin.mcinnes@glasgow.ac.uk.

patterns in an elliptical satellite ring, with peaks in density which can be used to provide enhanced coverage [10]. Letizia et al. [11] summarized the applications of PDE in astrodynamics, including interplanetary dust [7,8], nanosatellites [9] and high area-to-mass objects [12] to extend the continuity equation approach to multiple dimensions in phase space, defined by generic state variables, and then presented a procedure for the analytic solution to the continuity equation. McInnes [13] considered the orbital evolution of self-propelled 'smart dust' swarms in heliocentric orbit, and analytically derived the solutions to the continuity equation, including the evolution of an infinite sheet and a finite disk, evolution with on-orbit failures and with constant device deposition at one boundary. Most previous work builds on the natural evolution of passive bodies such as interplanetary dust [7,8], nanosatellites in constellations [9] and debris [6,13]. However, the self-propelled swarm discussed in this paper is assumed to be controllable by modulating the device pitch angle and lightness number. Active control of the evolution of the swarm becomes an interesting new problem for investigation.

Prior work on swarms has focused on the development of decentralised control laws which lead to desired emergent behaviour of multi-agent systems. For example, Punzo et al. [14] exploited a combination of artificial potential function methods and graph theory to control swarm shapes with reduced agent computational costs and improved robustness of the swarm. Later Punzo et al. [15] used the same method to control swarm formations with a self-similar central symmetry, which can generate fractal shapes for a distributed antenna array. Colombo et al. [16] developed a long-term orbit maintenance algorithm for satellite-on-a-chip or SpaceChip swarms based on the idea of balancing the energy dissipation from atmospheric drag with the energy gain from asymmetric solar radiation pressure. Izzo et al. [17] developed a decentralized formation-flying control architecture which produced homogeneous controllers able to plan the acquisition and maintenance of geometric formations. However, all such controllers developed for swarm control are derived from the ODEs of orbital dynamics, not from the PDEs of swarm density. As a quite different strategy from ODE control stabilizing finite-dimensional systems, most prior work on the stabilization of infinite-dimensional PDE models employ boundary controls to obtain a steady-state distribution [18,19]. This strategy can apply the PDE entropy function theorem [20] to build a candidate Lyapunov function and then design boundary controllers for distributed hyperbolic systems. However, the existence of such entropies are found only for homogeneous PDEs, which means that traditional boundary control is not available for the controlled evolution of swarms under on-orbit failures, with a non-homogeneous continuity equation.

In this paper, as an extension of Ref. [13], several control strategies to generate a required number density of a self-propelled 'smart dust' swarm are considered through a partial differential continuity equation. Again, building on Ref. [13], an azimuthally symmetric swarm is considered in **Section II** whose number density is a function of orbit radius and time only. According to the specific actuators providing control, the strategies developed are classified as a single-device and boundary controller, respectively. For the first type, provided by modulating a single device's lightness number and pitch angle, both open-loop and closed-loop forms are derived from the characteristic curves of the homogeneous continuity equation in **Section III.I**. For the second type, using active device deposition, both open-loop and closed-loop forms are derived by maintaining the required total number of devices in the swarm with on-orbit failures in **Section III.II**. Numerical simulations are implemented in **Section IV** which demonstrate that the combination of single-device and boundary controllers can drive the swarm number density to a required distribution, even considering on-orbit failures. It is also concluded that the controllers developed are robust with respect to uncertainty in the initial data used for the continuity equation.

II. Continuum Evolution Model of Swarm Density

A swarm of 'smart dust' devices distributed in heliocentric orbit is investigated by modelling the dynamical evolution of the swarm number density. Different from classical orbital dynamics formulated using ODEs, the swarm density is described by two independent variables of position and time, which requires the use of PDEs.

An azimuthally symmetric swarm model developed by McInnes [13] is considered whose number density is a function of orbit radius and time only. Similar to modelling the evolution of interplanetary dust [7,8], nano-satellite constellations [9] and high area-to-mass spacecraft [12,13], the continuum evolution of the swarm can be obtained from a continuity equation linking the swarm density and the velocity vector field of the flow of 'smart dust' devices, as [11]

$$\frac{\partial n}{\partial t} + \nabla \cdot (\boldsymbol{v} n) = \dot{n}^{+} - \dot{n}^{-} \tag{1}$$

where n represents the swarm density, ∇ is the gradient operator on the solution space, in this case the orbit radius $r(t)$, $\boldsymbol{v}$ is velocity vector of a single device, which is assumed a function of the orbit radius $r(t)$ only, and $\dot{n}^{+}$ and $\dot{n}^{-}$ represent the sources and the sinks of the PDE system which model the injection of new devices and the removal of devices due to on-orbit failures. Generally, the failure of devices will occur with a fixed probability such that

$$\dot{n}^{-} = -\eta \cdot n \tag{2}$$

where η>0 is the mean device failure rate. The realistic deposition of new devices is from a dispenser, defined here by the Dirac delta function as

$$\dot{n}^{+} = C\delta(r - \bar{r}) \tag{3}$$

where $\bar{r}$ represents the radius of the Earth's orbit and C is the deposition rate which is considered as a boundary controller in **Section III.II**.

The orbit evolution of a single device follows the model of Ref. [13] which is considered to be self-propelled by solar radiation pressure only. A new dimensionless dependent variable $\xi(t) = r(t)/\bar{r}$ and a new independent variable $\tau = \omega t$ are defined to simplify the analysis, where again $\bar{r}$ is the radius of the Earth's orbit, $\omega = \sqrt{\mu(1-\beta)/\bar{r}}$ is the orbital angular velocity, μ is the gravitational parameter and β is the device lightness number. It will be assumed that β can vary from 0.009 to 0.011, i.e., $\beta_0 - \Delta\beta \le \beta \le \beta_0 + \Delta\beta$ where β_0=0.01 and $\Delta\beta$=0.1·β_0, for example using an electrochromic coating. Thus, following Ref. [13], the evolution of a single device on a quasi-circular spiral trajectory is defined by the inward or outward radial speed

$$v_\xi = \frac{2}{3}\lambda(\alpha,\beta)\xi^{-1/2} \tag{4}$$

where the intermediate variable λ provides a link between the controllers developed in **Section III** and the controllable variables α and β, which, from Ref. [13] is given by

$$\lambda(\alpha,\beta) = \frac{3\beta}{1-\beta}\cos^2(\alpha)\sin(\alpha) \tag{5}$$

where $\alpha \in [-90^0, 90^0]$ is the pitch angle of the device relative to the Sun-line. The range of λ can then be defined as

$$-\frac{2}{\sqrt{3}}\frac{\beta_{\max}}{1-\beta_{\max}} \le \lambda(\alpha,\beta) \le \frac{2}{\sqrt{3}}\frac{\beta_{\max}}{1-\beta_{\max}} \tag{6}$$

where $\beta_{\max}=\beta_0+\Delta\beta$.·Both α and β are considered as the two control variables to drive the actual swarm number density $n(\xi)$ to some required distribution $n_{req}(\xi)$ asymptotically at infinite time. Therefore, again following Ref. [13], the continuum evolution of the density defined by Eq. (1) can be simplified as

$$\frac{\partial n}{\partial \tau} + v_\xi \frac{\partial n}{\partial \xi} + n(\xi,\tau)\left(\frac{v_\xi'}{v_\xi} + \frac{1}{\xi}\right) = \dot{n}^{+} - \dot{n}^{-} \tag{7}$$

where (′) is defined as differentiation with respect to ξ. If both the source and sink terms are ignored in this equation, it is referred as the homogeneous evolution model.

Solutions to the continuum evolution equation can be achieved by propagating the initial data for the swarm forward to describe the evolution of n as a function of both ξ and τ. The initial data function is defined as $n_0(\xi) = n(\xi,\tau)|_{\tau=0}$, which is taken as a constant $n_0(\xi)=1$ for illustration in Refs. [9,13]. According to **Section III.I**, the analytic solution to the homogeneous model depends on the specific initial data function $n_0(\xi)$. An extension of the constant initial data is achieved in this paper by introducing an example radius-dependent initial data $n_0(\xi)$ with the following form

$$n_0(\xi) = 1 + \kappa \cdot \cos(2\pi \cdot \xi) \tag{8}$$

where κ is a free parameter denoting the difference from the original initial data with $n_0(\xi)=1$ used in Ref. [13]. For numerical implementation, a finite limit on ξ is defined, such as $\xi \in (0,1]$.

As demonstrated in **Section III**, both open-loop and closed-loop controllers define the selection of the intermediate variable λ for any radius ξ and time τ. Then, another algorithm is required to choose a pair of (α, β) from the constraint defined Eq. (5). From the viewpoint of optimization, an optimization index is defined as

$$J = \gamma\alpha^2 + (\beta - \beta_0)^2 \tag{9}$$

where γ is the weighting factor between α and β. Therefore, the procedure for obtaining α and β from $\lambda|_{\xi,\tau}$ at any radius and time can be classified as a nonlinear constrained optimization with Eq. (5) as the constraint such that

$$\left.\begin{array}{c} \min J \\ s.t., \lambda(\alpha,\beta) = \lambda|_{\xi,\tau} \\ -\frac{\pi}{2} \le \alpha \le \frac{\pi}{2} \\ \beta_0 - \Delta\beta \le \beta \le \beta_0 + \Delta\beta \end{array}\right\} \tag{10}$$

where the functions “fmincon” and “confuneq” in MATLAB® can deal with such optimizations, providing the actual controls required as a function of both radius and time.

III. Control Strategies for the Evolution of Swarm Density

Different types of passive swarms have been investigated, such as nanosatellites by McInnes [9] and McInnes and Colombo [10], and debris by Letizia et al [11]. However the smart dust devices considered in this paper are assumed to be actively controlled through modulation of their lightness number β and pitch angle α defined by Eq. (5). Furthermore, since all devices are assumed to be active rather than passive, a required distribution of swarm density can in principle be delivered through open-loop or closed-loop controllers, developed in **Section III.I**.

Moreover, the device deposition strategies proposed in **Section III.II** are considered to compensate for on-orbit failures, which act as a boundary controller in the classical PDE control problem. Compared with the active device controllers for individual devices in **Section III.I**, the boundary control is provided by the macroscopic deposition of new devices.

III.I. Open-loop and Closed-loop Device Controllers for a Homogeneous Continuity Equation

Analytic closed-form solutions to the continuity equation modelling the evolution of nanosatellite constellations [9,10], high area-to-mass objects [12] and 'smart dust' in heliocentric orbit can be derived using the method of characteristics. Thus, the standard method proposed by McInnes [13] is introduced to investigate the evolution of a swarm in heliocentric orbit.

Firstly, considering the homogeneous case with a sink term $\dot{n}^{-}(\xi,\tau)=0$ and source term $\dot{n}^{+}(\xi,\tau)=0$, the motion of a single device defined by Eq. (4) allows simplification of the partial differential Eq. (7) as

$$\frac{\partial n}{\partial \tau}+\frac{2}{3}\lambda(\alpha,\beta)\xi^{-\frac{1}{2}}\cdot\frac{\partial n}{\partial \xi}+\frac{1}{3}\lambda(\alpha,\beta)\xi^{-\frac{3}{2}}\cdot n(\xi,\tau)=0 \tag{11}$$

Along the characteristic curves, the partial differential equation degenerates into two ordinary differential equations defined by [21]

$$\frac{d\xi}{d\tau}=v_{\xi} \tag{12}$$

$$\frac{dn}{d\xi}+\frac{1}{2\xi}n(\xi,\tau)=0 \tag{13}$$

Then, substituting from Eq. (4) yields the family of characteristic functions $G(\xi,\tau)$ defined by

$$G(\xi,\tau)=\xi^{\frac{3}{2}}-\int_0^{\tau}\lambda(\alpha,\beta)d\tau\,. \tag{14}$$

Therefore, the general solution of the original partial differential equation can be written as

$$n(\xi,\tau)=\xi^{-\frac{1}{2}}e^{\psi[G(\xi,\tau)]} \tag{15}$$

where an arbitrary function of the characteristic equation ψ can be determined from the initial data (or function) of the problem $n_0(\xi)=n(\xi,\tau)\big|_{\tau=0}$, i.e., ψ has the following form $\psi\left(\xi^{\frac{3}{2}}\right)=\ln\left[\left(\xi^{\frac{3}{2}}\right)^{\frac{1}{3}}n_0\left(\left(\xi^{\frac{3}{2}}\right)^{\frac{2}{3}}\right)\right]$. Thus, substituting the characteristic function $G(\xi,\tau)$ and ψ into the density defined by Eq. (15) yields the full swarm density equation as

$$n(\xi,\tau)=\left[1-\frac{1}{\xi^{3/2}}\int_0^{\tau}\lambda(\alpha,\beta)d\tau\right]^{\frac{1}{3}}\cdot n_0(\zeta) \tag{16}$$

where $\zeta=\left[\xi^{3/2}-\int_0^{\tau}\lambda(\alpha,\beta)d\tau\right]^{\frac{2}{3}}$. The full density equation will now contribute to the derivation of both the open-loop and closed-loop controllers for the swarm of devices. The required distribution of swarm density $n_{req}(\xi)$, which depends on orbit radius only, and defines the control target of both controllers discussed above, is defined as $n(\xi,\tau)\xrightarrow{\tau\to+\infty}n_{req}(\xi)$.

To proceed with the analysis, an intermediate variable is defined as $\phi(\xi)=\xi^{\frac{3}{2}}-\int_0^{+\infty}\lambda(\alpha,\beta)d\tau$, and then the relationship between this variable and the required density distribution $n_{req}(\xi)$ is obtained according to Eq. (16) as

$$\phi(\xi)^{\frac{1}{3}}\cdot n_0\left[\phi(\xi)^{\frac{2}{3}}\right]=\xi^{\frac{1}{2}}\cdot n_{req}(\xi) \tag{17}$$

which can be defined as $y=x\cdot n_0(x^2)$, where the variables x and y are replaced by $\phi(\xi)$ and $\xi^{\frac{1}{2}}\cdot n_{req}(\xi)$. The inverse function of $y=x\cdot n_0(x^2)$ is denoted as $x=g(y)$ (a Newton iteration algorithm to solve this equation is presented in the **Appendix**), and $\phi(\xi)$ can be solved as $\phi(\xi)^{\frac{1}{3}}=g\left(\xi^{\frac{1}{2}}\cdot n_{req}(\xi)\right)$ or $\phi(\xi)=\left[g\left(\xi^{\frac{1}{2}}\cdot n_{req}(\xi)\right)\right]^3$. The relationship between λ and ξ and τ is therefore obtained as

$$\int_0^{+\infty}\lambda(\alpha,\beta)d\tau=\xi^{3/2}-\phi(\xi) \tag{18}$$

To solve for the term λ in the above relationship, several candidate functions $\lambda(\tau)$ satisfying a condition based on the finite nature of $\int_0^{+\infty}\lambda(\tau)d\tau$ and $\lambda(+\infty)$ can be used to deal with the infinite integral. For example a form $\int_0^{+\infty}\frac{K_1}{1+K_1^2\tau^2}d\tau=\arctan K_1\tau\Big|_0^{+\infty}$ (or $\int_0^{+\infty}\frac{K_1}{(1+K_1\tau)^2}d\tau=\frac{-1}{1+K_1\tau}\Big|_0^{+\infty}$) will be employed in this paper. Therefore, one form of the open-loop control can be found as

$$\lambda(\alpha,\beta)=\frac{2}{\pi}\cdot\frac{\xi^{3/2}-\phi(\xi)}{1+K_1^2\tau^2}K_1 \tag{19}$$

where $K_1>0$ can be used to accelerate or decelerate the convergence rate of the density $n(\xi,\tau)$ to the required density $n_{req}(\xi)$. Here $\lambda(\alpha,\beta)$ is monotonically increasing (when $\xi^{3/2}<\phi(\xi)$) or decreasing (when $\xi^{3/2}>\phi(\xi)$) with respect to time τ.

Thus, the absolute value of $\lambda(\alpha,\beta)$ reaches its maximum at τ=0, which cannot be beyond the boundary of λ defined by Eq. (6). Thus, it can be shown that

$$K_1 \le \frac{\pi}{\sqrt{3}} \frac{\beta_{\max}}{1-\beta_{\max}} \cdot \frac{1}{\left|\xi^{3/2} - \phi(\xi)\right|} \tag{20}$$

where $\phi(\xi)^{\frac{1}{3}} = g\left(\xi^{\frac{1}{2}} \cdot n_{req}(\xi)\right)$.

To check the stability of the open-loop control, Eq. (19) is substituted into the full swarm density Eq. (16) and then the limit of $n(\xi,\tau)$ at $\tau \to +\infty$ is derived as

$$\lim_{\tau\to+\infty} n(\xi,\tau) = \left[1 - \frac{1}{\xi^{3/2}} \int_0^{+\infty} \frac{2K_1}{\pi} \cdot \frac{\xi^{3/2} - \phi(\xi)}{1+K_1^2\tau^2} d\tau\right]^{\frac{1}{3}} n_0\left(\left[\xi^{3/2} - \int_0^{+\infty} \frac{2K_1}{\pi} \cdot \frac{\xi^{3/2} - \phi(\xi)}{1+K_1^2\tau^2} d\tau\right]\right) = \xi^{-1/2}\phi(\xi)^{1/3} n_0\left[\phi(\xi)^{1/3}\right] \tag{21}$$

According to the relationship between $\phi(\xi)$ and $n_{req}(\xi)$ defined by Eq. (17), it is concluded that $\lim_{\tau\to+\infty} n(\xi,\tau) = n_{req}(\xi)$, which demonstrates the asymptotic stability of the open-loop control.

Compared with the open-loop control, closed-loop control is expected to reduce the control error through feedback from the deviation of actual and required density distributions $n(\xi,\tau) - n_{req}(\xi)$ at the current time τ. Another intermediate variable is then defined as

$$\varphi(\xi,\tau) = \left[\xi^{\frac{3}{2}} - \int_0^{\tau} \lambda(\alpha,\beta) d\tau\right]^{1/3} \tag{22}$$

which can be used to transform Eq. (16) into another form as

$$\varphi \cdot n_0\left(\varphi^2\right) = \xi^{\frac{1}{2}} n(\xi,\tau) \tag{23}$$

According to the algorithm presented in the Appendix, the intermediate variable φ can be solved from Eq. (23) as a function of $\xi^{\frac{1}{2}} n(\xi,\tau)$ denoted as

$$\varphi = g\left(\xi^{\frac{1}{2}} n(\xi,\tau)\right) \tag{24}$$

and is then substituted into Eq. (22) to yield

$$\left[g\left(\xi^{\frac{1}{2}} n(\xi,\tau)\right)\right]^3 = \xi^{\frac{3}{2}} - \int_0^{\tau} \lambda(\alpha,\beta) d\tau \tag{25}$$

Thus, differentiating Eq. (25) with respect to time τ only it can be shown that

$$\frac{d}{d\tau}\left(\left[g\left(\xi^{\frac{1}{2}}n(\xi,\tau)\right)\right]^3-\left[g\left(\xi^{\frac{1}{2}}n_{req}(\xi)\right)\right]^3\right)=-\lambda(\alpha,\beta) \tag{26}$$

where the term $\left[g\left(\xi^{\frac{1}{2}}n_{req}(\xi)\right)\right]^3$ is independent of time τ and can be added into the differentiation.

Then, for a coefficient K_2>0, the closed-loop control can be determined from Eq. (26) to ensure convergence to the required swam density so that

$$\lambda(\alpha,\beta)=K_2\cdot\left(\left[g\left(\xi^{\frac{1}{2}}n(\xi,\tau)\right)\right]^3-\left[g\left(\xi^{\frac{1}{2}}n_{req}(\xi)\right)\right]^3\right) \tag{27}$$

and by analogy with a damped first order system for some variable x, $\dot{x}=-K_2x$, where again K_2>0 can be used to accelerate or decelerate the convergence rate of the density $n(\xi,\tau)$ to the required density $n_{req}(\xi)$. Due to the fact that $x=e^{-K_2\cdot\tau}x_0\le x_0$, $\lambda(\alpha,\beta)$ reaches its extremum at τ=0, which cannot be beyond the boundary of λ defined by Eq. (6). Thus, it can be shown that

$$K_2\cdot\le\frac{2}{\sqrt{3}}\frac{\beta_{\max}}{1-\beta_{\max}}\cdot\frac{1}{\left|\left[g\left(\xi^{\frac{1}{2}}n_0(\xi)\right)\right]^3-\left[g\left(\xi^{\frac{1}{2}}n_{req}(\xi)\right)\right]^3\right|}\cdot \tag{28}$$

To prove the asymptotic stability of the closed-loop control by the Lyapunov method, the following Lyapunov function is defined as

$$V(\tau)=\frac{1}{2}\left[n(\xi,\tau)-n_{req}(\xi)\right]^2 \tag{29}$$

Cleary, $V(\tau)$ is always non-negative. Combining Eqs. (22) and (24) then yields

$$\xi^{\frac{3}{2}}-\int_0^\tau\lambda(\alpha,\beta)d\tau=\left[g\left(\xi^{\frac{1}{2}}n\right)\right]^3 \tag{30}$$

and so differentiating with respect to time yields

$$-\lambda(\alpha,\beta)=3g^2g'\cdot\xi^{\frac{1}{2}}\frac{\partial n}{\partial\tau} \tag{31}$$

The time-derivative of the Lyapunov function therefore becomes

$$\dot{V}(\tau)=\left[n(\xi,\tau)-n_{req}(\xi)\right]\frac{\partial n}{\partial\tau} \tag{32}$$

Substituting Eq. (31) into (32) yields

$$\dot{V}(\tau)=-\frac{1}{3g^2g'\xi^{\frac{1}{2}}}\left[n(\xi,\tau)-n_{req}(\xi)\right]\cdot\lambda(\alpha,\beta) \tag{33}$$

and substituting Eq. (27) into (33) yields

$$\dot{V}(\tau) = -\frac{K_2}{3g^2 g' \xi^{\frac{1}{2}}} \left[n(\xi,\tau) - n_{req}(\xi) \right] \cdot \left(\left[g\left(\xi^{\frac{1}{2}} n(\xi,\tau) \right) \right]^3 - \left[g\left(\xi^{\frac{1}{2}} n_{req}(\xi) \right) \right]^3 \right) \tag{34}$$

To make sure $\dot{V}(\tau)$ is negative always, the inverse function $g(\cdot)$ of $y = x \cdot n_0(x^2)$, i.e., $x = g(y)$, defined in the Appendix, is expected to be monotonically increasing or decreasing (increasing in this paper). Thus, differentiating $y = x \cdot n_0(x^2)$ with respect to x and combining with the requirement $\frac{dy}{dx} > 0$ yields $n_0(x^2) + 2x^2 \cdot \frac{dn_0(x^2)}{d(x^2)} > 0$. Since $n_0(\xi)$ depends on ξ only, replacing x^2 by ξ yields

$$\frac{n_0(\xi)}{\xi} + 2 \cdot \frac{dn_0(\xi)}{d\xi} > 0 \cdot \tag{35}$$

For the initial data used in this paper defined by Eq. (8), it can be shown from the above condition that

$$1 + \kappa \cdot \sqrt{1 + 4\pi^2 \xi^2} \cos(2\pi \cdot \xi + \vartheta) > 0 \tag{36}$$

where $\vartheta = \arctan(4\pi\xi)$. Thus, any of $\kappa \in \left(-\frac{1}{\sqrt{1+4\pi^2}}, \frac{1}{\sqrt{1+4\pi^2}} \right) \subset \left(-\frac{1}{\sqrt{1+4\pi^2\xi^2}}, \frac{1}{\sqrt{1+4\pi^2\xi^2}} \right)$ will ensure the monotonic property of $g(\cdot)$.

It is clear from the monotonic property of $g(\cdot)$ that $\dot{V}(\tau)$ is negative always expect for $n(\xi,\tau)=n_{req}$. Therefore, the boundedness of the control error is rigorously proven by the Lyapunov theorem.

III.II. *Boundary Control for On-orbit Failures*

Due to the fact that on-orbit failures within a swarm will decrease the total number of devices, new devices should be supplied to the swarm to maintain the required distribution. Thus, according to the definition of swarm number density given by McInnes [9,13], the total number of swarm devices is defined as

$$N(\tau) = \int_{\varepsilon_1}^{1} 2\pi\xi \cdot n(\xi,\tau) d\xi \tag{37}$$

where $\varepsilon_1 > 0$ is chosen to avoid a singular integral, where $\varepsilon_1 = 0.01$ in this paper.

The sink term $\dot{n}^- = -\eta \cdot n(\xi,\tau)$ in Eq. (7) represents on-orbit failures and will decrease the total number of devices in the swarm, where $1/\eta$ is the mean device failure rate. To keep the required distribution $n_{req}(\xi)$, new devices should be supplied by deposition, assumed from the Earth's orbit at $\xi = 1$, i.e.

$$\dot{n}^+ = C \cdot \delta(\xi - 1) \tag{38}$$

where δ is the Dirac delta function, and C is some undetermined coefficient. Thus, the source term $\dot{n}^+$ works as a boundary controller to deal with on-orbit failures.

Therefore, the stabilization by both active device control and boundary deposition is similar to water flowing into a pond $\xi \in (0,1]$ where $\dot{n}^-$ is analogous to continuous evaporation and $\dot{n}^+$ is analogous to a tap placed at unit radius $\xi = 1$. The swarm will flock together at $\xi = 1$ but 'dry up' at other radii without the active control through the term $\lambda(\alpha,\beta)$. Thus, the device controllers developed in **Section III.I** work as a 'water pump' to drive the swarm number density to the required density.

Similar to the control strategies developed for a single device, the boundary control for device deposition includes open-loop and closed-loop strategies. When the swarm reaches the required distribution $n_{req}(\xi)$ at $\tau \to +\infty$, the first term $\partial n/\partial \tau$ in Eq. (7) tends to zero, as well as other terms in the device controllers, and the source and sink terms are expected to be in balance such that $\dot{N}(\tau) = \int_{\varepsilon_1}^{1} 2\pi\xi \cdot (\dot{n}^+ - \dot{n}^-) d\xi = 0$. The magnitude of the source term can therefore be defined as

$$\tilde{C} = \eta \int_{\varepsilon_1}^{1} \xi \cdot n_{req}(\xi) d\xi \tag{39}$$

A closed-loop strategy can then be derived based on the idea of eliminating the difference between the total number at any moment $N(\tau)$ and the required total number. Thus, as a feedback of the current total number of devices in the swarm $N(\tau)$, the magnitude of the source term can be defined as

$$C(\tau) = \tilde{C} + K_3 \cdot [N(\tau) - N_{req}] = \tilde{C} + K_3 \cdot 2\pi \int_{\varepsilon_1}^{1} \xi \cdot [n(\xi,\tau) - n_{req}(\xi)] d\xi \tag{40}$$

where $K_3<0$ can again be used to accelerate or decelerate the convergence rate of the density $n(\xi,\tau)$ to the required density $n_{req}(\xi)$.

It is found to be quite difficult to maintain the total number N during stabilization due to the errors between the actual and required densities. Instead, a balancing state is achieved through the sink and source terms so that the rate of change of the total number of devices is zero, i.e., the total number of devices is stable, but not necessarily equal to the initial number of devices.

IV. Numerical Simulations

Numerical simulations are now implemented to evaluate the effectiveness of both the single device and deposition controllers developed in **Section III**, of which the significant parameters are set as follows. Firstly, the parameter κ of the initial data function n_0 is taken as 0.01 in most of scenarios, except for numerical investigations on robustness with respect to the initial data. For numerical implementation, a finite limit on ξ is defined, such that $\xi \in (0,1]$. Secondly, the tolerance value ε_2 of the iteration algorithm proposed in the Appendix is selected as 1×10^{-7}. Thirdly, the on-orbit failure rate is set as $\eta=1\times10^{-3}$ for the failure case. Fourthly, according to the boundaries of the control gains presented in **Section III.I**, the gains of open-loop and closed-loop device controllers and the closed-loop boundary controller are chosen as K_1=0.04, K_2=0.04 and K_3= −0.8, respectively. Then, the finite difference method is employed to solve the partial differential equation Eq. (7) numerically, where the simulation steps of time and radius are set as 1×10^{-2} and 1×10^{-3}, respectively. Moreover, to assess the control error of the controllers, the relative error of number density is defined as

$$e(\xi)=\lim_{\tau\to+\infty}\frac{\left|n(\xi,\tau)-n_{req}(\xi)\right|}{n_{req}(\xi)}. \tag{41}$$

where a 15 year integration time is adopted.

Distributed swarms have potential applications in providing simultaneous multi-point solar field and particle measurements and so a uniform number density can be used $n(\xi,0)=1$, i.e., $\kappa=0$, as adopted by McInnes [9,13]. However, as a non-uniform test case a distribution with peaks at the two inferior planets, i.e., Mercury and Venus, is adopted, shown as the red dashed line in Fig.1. By polynomial fitting, the blue solid line will provide the required distribution $n_{req}(\xi)$ to drive the stabilization of the swarm number density using the proposed controllers.

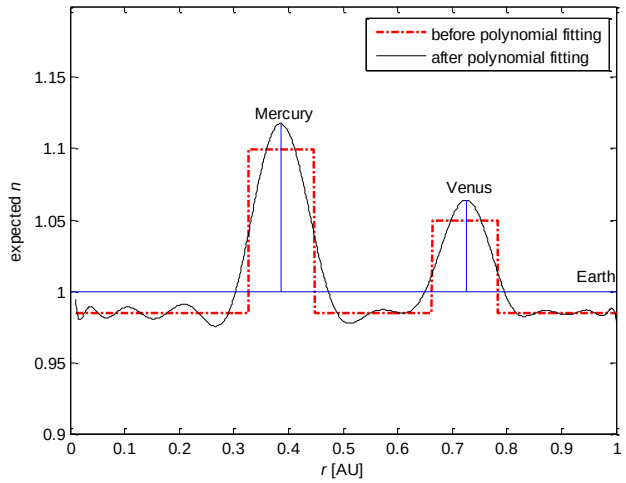

Fig.1 Required distributions by polynomial fitting.

For the homogeneous case, stabilization by both the open-loop and closed-loop device controllers presented in **Section III.I** is demonstrated in Figs. 2 and 3 respectively. The relative errors of number density are illustrated in Fig.4. The maximum relative error of the closed-loop controller is 3%, but the maximum relative error of the open-loop controller is 4.5%. Thus, it can be seen that the closed-loop controller has a better performance than the open-loop control, as expected, due to feedback from the current number density. Therefore, only the closed-loop device controller is used in the following section to stabilize the swarm with on-orbit failures using the boundary controller proposed in **Section III.II**.

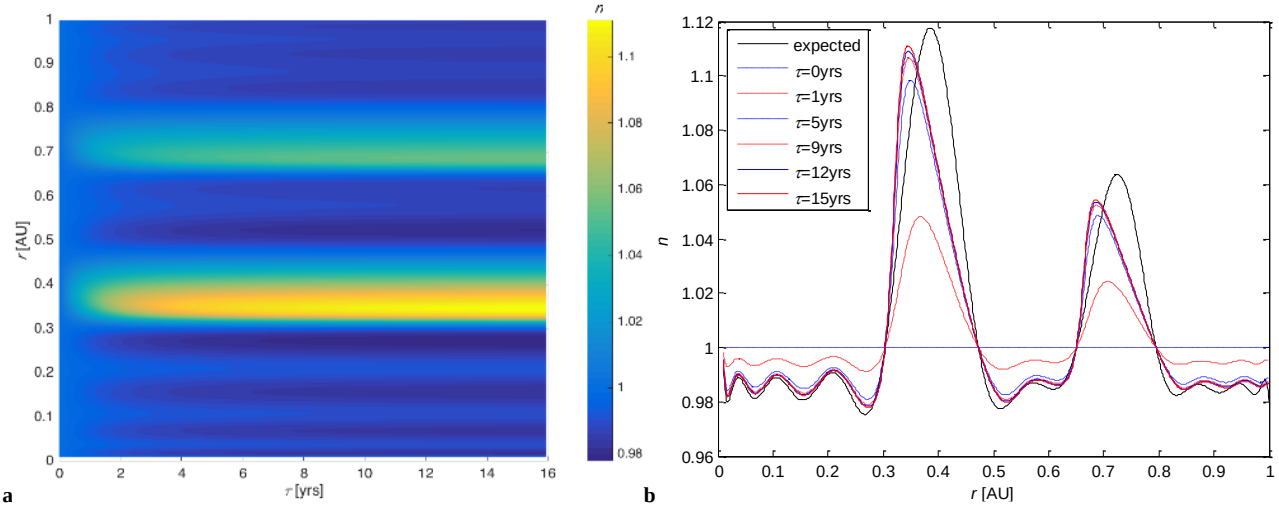

a **b**

Fig.2 Stabilization by open-loop device controller for homogeneous case: **a** full evolution by open-loop controller; **b** evolution at time steps.

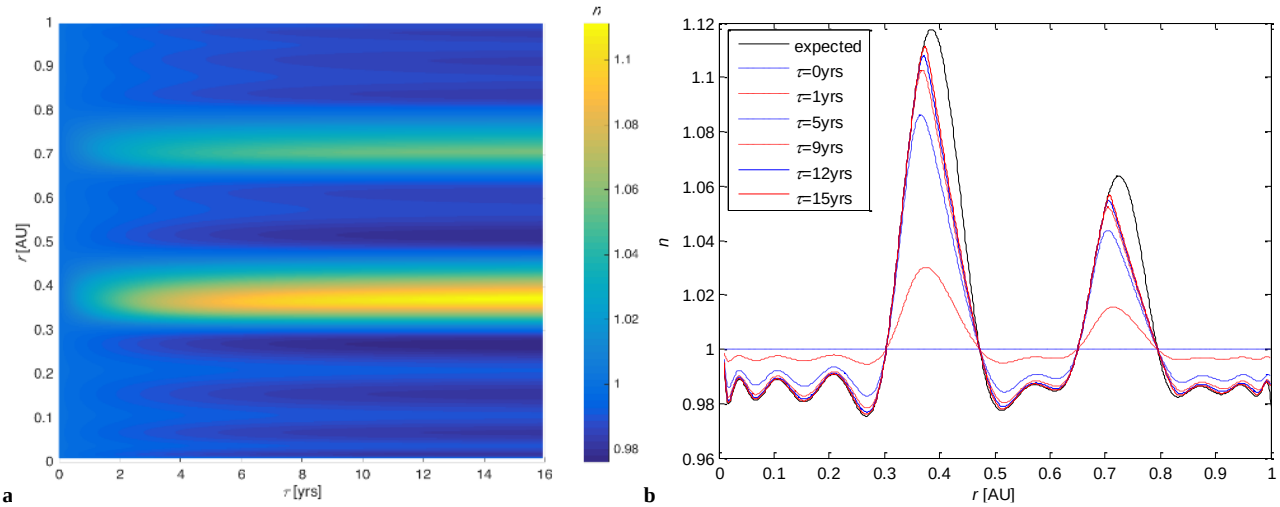

a **b**

Fig.3 Stabilization by closed-loop device controller for homogeneous case: **a** full evolution by closed-loop controller; **b** evolution at time steps.

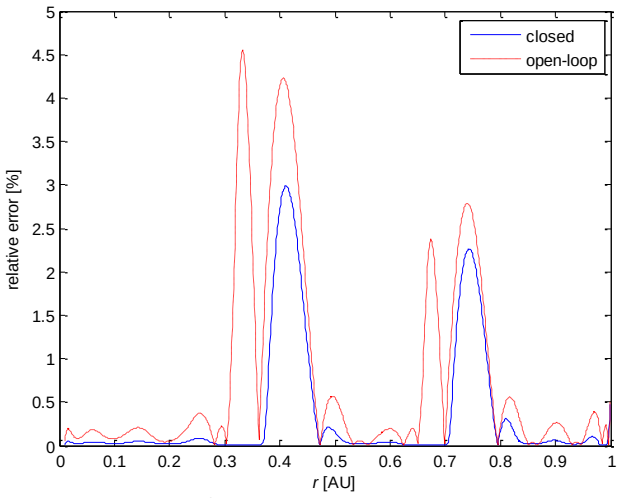

Fig.4 Relative errors of number density.

The values of α and β provided by the closed-loop device controller can be found from the optimization procedure presented in **Section II**, and is shown in Figs. 5 and 6 for different weighting factors. When the relative weighting factor is selected as γ=0, the value of α varies from -10^0 to 4^0, and β is equal to 0.01; when the weighting factor is selected as γ=50, the value of α varies from -9^0 to 3.8^0, and the value of β varies from 0.01 to 0.011. Thus, compared with the weighting factor γ=0 with fixed β, i.e., β_0, a larger weighting γ=0.02 with variable β can reduce the rate of change of α. Thus, the optimized control allocations of lightness number and pitch angle show slow rates of change of α and β to make the stabilization strategies realizable.

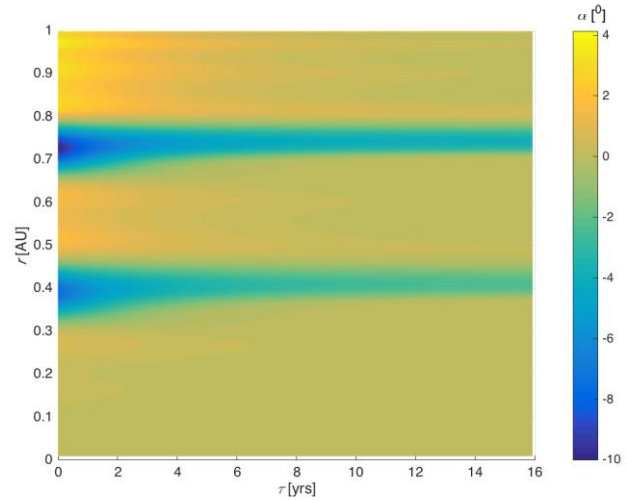

Fig.5 Evolution of the pitch angle α provided by the closed-loop device controller (γ=0).

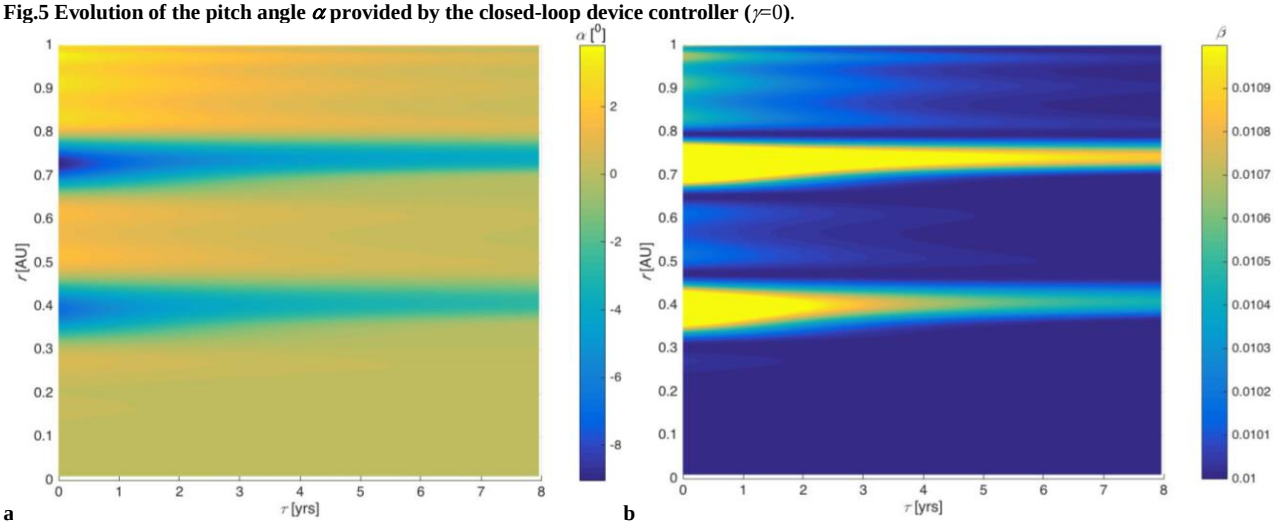

a **b**

Fig.6 Evolution of the pitch angle α and lightness number β provided by the closed-loop device controller (γ=0.02).

Considering on-orbit failures, the evolution and relative error of the stabilized distribution obtained by the combination of closed-loop device control and open-loop boundary control is demonstrated by the red dashed lines in Figs.7a and 7c, as well as the combination of closed-loop device and closed-loop boundary control illustrated by the solid blue line in Figs.7a and 7c. It can be seen that the combination of closed-loop device and closed-loop boundary control has a better performance with a maximum relative error of 6% compared with 8% for the other combination, and works better at maintaining the total number of devices in the swarm. It can also be seen that the device controllers will fail in stabilizing on-failures without the help of the open-loop or closed-loop boundary controller.

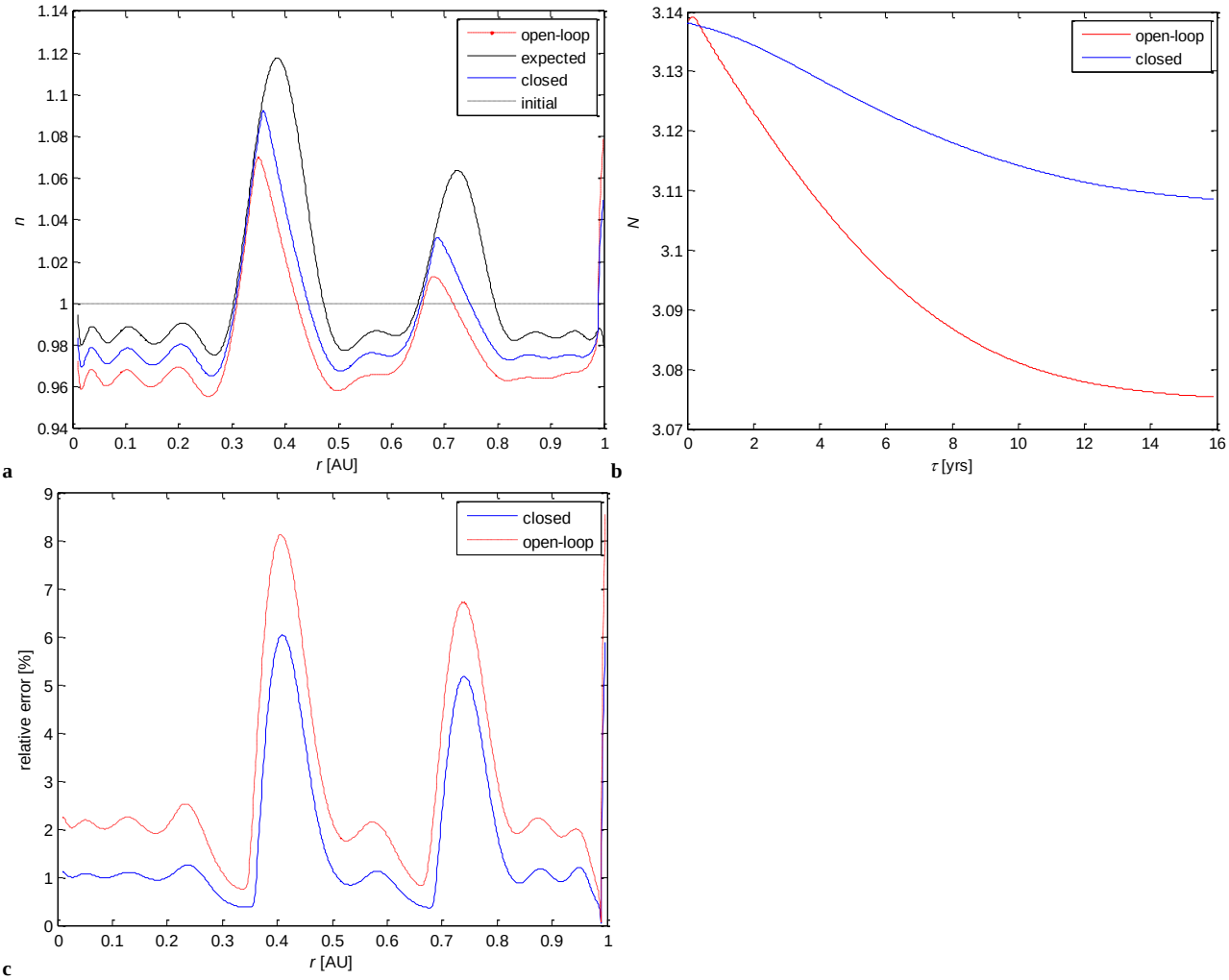

Fig.7 **Evolution of stabilized number density for on-orbit failures case**: **a** the evolution of stabilized distributions at year 15; **b** the time histories of the total number of devices in the swarm; **c** the relative errors of the stabilized distributions.

According to the derivation of the closed-loop device controller in **Section III.I**, the form of the controller depends on the initial data. Thus, it is necessary to investigate the robustness of the controller with respect to the parameter κ of the initial data function. The closed-loop device controller in the following simulation is based on $\kappa = 0.01 \in \left(-\frac{1}{\sqrt{1+4\pi^2}}, \frac{1}{\sqrt{1+4\pi^2}} \right)$, while the actual values of initial data are set as κ=0.01, 0.1, 0.2, 0.3, 0.4, respectively. Using the same controller, the relative errors of the stabilized density in the different scenarios parameterized by κ are shown in Fig.8. The maximum relative errors stabilized by the designed controller under the actual initial data parameter κ=0.01 is 3%, the maximum under the parameter κ=0.1 is 5%, the maximum under the parameter κ=0.2 is 11%, the maximum under the parameter κ=0.3 is 16%, and the maximum under the parameter κ=0.4 is 22%. Thus, it is can be seen that the controller developed is robust with respect to small variations in the initial data.

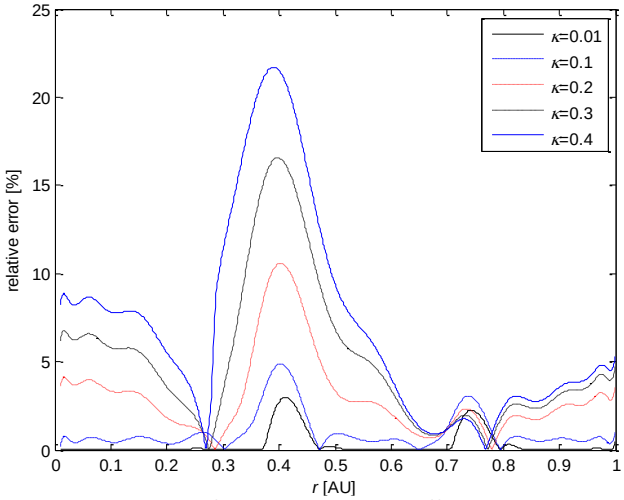

Fig.8 Relative Errors of stabilized density in different initial data scenarios year 15.

V. Conclusion

Distributed 'smart dust' swarms have potential applications in providing simultaneous multi-point field and particle measurements through self-propelled micro-electromechanical-system (MEMs)-scale devices in heliocentric orbit. The orbital evolution of the number density of such a swarm was investigated by a continuity partial differential equation (PDE), instead of an ordinary differential equation (ODE), with stabilization strategies investigated to drive the swarm to some required number density distribution. Due to solar radiation pressure (SRP), the single-device controller provided the required lightness number and pitch angle which were derived from the characteristic curves of the homogeneous system; however, a boundary control provided by the deposition of new devices was also derived from the total number of devices in the swarm. The former works as a 'water pump' to drive the swarm number density and its required distribution, while the latter acts as a 'water pump' at Earth orbit to supply new devices to offset on-orbit failures.

Thus, rather than a uniform distribution, a non-uniform distribution was adopted with peaks in density at Venus and Mercury as an example in this paper. The four stabilization strategies for the swarm number density distribution developed, i.e., the open-loop and closed-loop controllers for the homogeneous system and the open-loop and closed-loop controls for the nonhomogeneous system, can drive the swarm to any required distribution with control errors of 3%, 4.5%, 6% and 8%, respectively. The closed-loop controllers with asymptotic stability achieve smaller errors than the open-loop ones. Due to the constraints on the device lightness number and attitude angle, the selections of control gains are derived analytically as well as the selection of the two parameters α *and* β by an optimization technique. It was demonstrated numerically that the controllers are robust with respect to variations in the initial data, even if the controller depends on the initial data itself.

Acknowledgments

Ming Xu acknowledges support from the Fundamental Research Funds for the Central Universities and China Scholarship Council program (201506025138), and Colin McInnes acknowledges the support of a Royal Society Wolfson Research Merit Award.

References

[1] Bewick, R., Lücking, C., Colombo, C., Sanchez Cuartielles, J.P., and McInnes, C. R., "Heliotropic dust rings for Earth climate engineering", *Advances in Space Research*, Vol. 51, No. 7, 2013, pp. 1132-1144.
doi:10.1016/j.asr.2012.10.024

[2] Nicola J., "Tiny 'chipsat' spacecraft set for first flight", *Nature*, Vol. 534, 2016, pp. 15-16.

[3] Colombo, C., and McInnes, C., "Orbit design for future SpaceChip swarm missions in a planetary atmosphere", *Acta Astronautica*, Vol. 75, 2012, pp. 25-41.
doi: j.actaastro.2012.01.004

[4] Lorraine M. W., Mason P., "Chip-Scale Satellite Control with Multiple Electrodynamic Tethers", *Journal of Guidance, Control, and Dynamics*, Vol.39, 2016, pp. 1643-1646.
doi: 10.2514/1.G001438

[5] Heard W. B., "Dispersion of ensembles of non-interacting particles", *Astrophysics and Space Science*, Vol. 43, 1976, pp. 63-82.

[6] McInnes C. R., "An analytical model for the catastrophic production of orbital debris", *ESA Journal*, Vol. 17, 1993, pp. 293-305.

[7] Gor'kavyi N., et al, "A new approach to dynamical evolution of interplanetary dust", *The Astrophysical Journal*, Vol. 474, 1997, pp. 496-502.
doi: 10.1086/303440

[8] Gor'kavyi N., et al, "Quasi-stationary states of dust flows under Poynting-Robertson drag: New analytical and numerical solutions", *The Astrophysical Journal*, Vol. 488, 1997, pp. 268-276.

[9] McInnes C. R., "A simple analytic model of the long term evolution of nanosatellite constellations", *Journal of Guidance, Control, and Dynamics*, Vol. 23, No. 2, 2000, pp. 332-338.
doi: 10.2514/2.4527

[10] McInnes C. R., Colombo C., "Wave-like patterns in an elliptical satellite ring", *Journal of Guidance, Control, and Dynamics*, Vol. 36, No. 6, 2013, pp. 1767-1771.
doi: 10.2514/1.55956

[11] Letizia F., Colombo C., Lewis H., "Multidimensional extension of the continuity equation method for debris clouds evolution", *Advances in Space Research*, Vol. 57, No. 8, 2015, pp. 1-17.

doi: 10.1016/j.asr.2015.11.035

[12] Colombo C., McInnes C. R., "Evolution of swarms of smart dust spacecraft", New Trends in Astrodynamics and Applications VI, Courant Institute of Mathematical Sciences, New York, 2011.

[13] McInnes C. R., "A Continuum Model for the Orbit Evolution of Self-propelled “Smart Dust” Swarms", *Celestial Mechanics and Dynamical Astronomy*, 2016, Vol. 124, No. 4, pp. 501-517, 2016.

[14] Punzo G., Bennet J. D., Macdonald M., "Swarm shape manipulation through connection control", Proceedings of TAROS 2010 - Towards Autonomous Robotic Systems, 2010.

[15] Punzo G,, Karagiannakis P., Bennet J. D., Macdonald M., Weiss S., "Enabling and exploiting self-similar central symmetry formations", *IEEE Transactions on A*erospace *and Electronic Systems*, Vol. 50, No. 1, 2014, pp. 689-703.
doi: 10.1109/TAES.2013.120074

[16] Colombo C., Lucking C., McInnes C. R., "Orbit evolution, maintenance and disposal of SpaceChip swarms through electro-chromic control", *Acta Astronautica*, Vol. 82, No. 1, 2013, pp. 25-37.
doi: 10.1016/j.actaastro.2012.05.035

[17] Izzo D., Simoes F. L., et al, "An evolutionary robotics approach for the distributed control of satellite formations", *Evolutionary Intelligence*, Vol. 7, No. 2, 2014, pp. 107-118.
doi: 10.1007/s12065-014-0111-9

[18] Coron J. M., et al, "On boundary control design for quasilinear hyperbolic systems with entropies as Lyapunov functions", Proceedings of the 41rt IEEE Conference on Decision and Control Las Vegas, Nevada USA, 2002.

[19] van den Berg R A, "Partial differential equations in modelling and control of manufacturing systems", Master’s thesis, Eindhoven University of Technology, 2004.

[20] Serre D., Systèmes de lois de conservations. Diderot éditeur, Art et Sciences, 1996, Chap. 4.

[21] Murphy, I .S., “Advanced Calculus”, Arklay Publishers, Stirling, 1984, pp. 79-101.

VI. Appendix

A Newton iteration algorithm to obtain $\phi(\xi)^{\frac{1}{3}}$ from $\phi(\xi)^{\frac{1}{3}} \cdot n_0\left[\phi(\xi)^{\frac{2}{3}}\right] = \xi^{\frac{1}{2}} \cdot n_{req}(\xi)$ in Eq. (16) or to obtain φ from $\varphi \cdot n_0(\varphi^2) = \xi^{\frac{1}{2}} n$ in Eq. (22) is essentially that to solve the zero root of the equation $f(x) = x \cdot n_0(x^2) - y$, where it is assumed that the function n_0 is close to 1:

1) Due to the fact that the function n_0 is close to 1, the root in the first iteration can be chosen as y, i.e., $x_1 = y$;
2) Substitute the root in the k^{th} iteration in the equation $f(x_k) = x_k \cdot n_0(x_k^2) - y$;

3) Define the correction to x_k as Δ to make the k+1th iteration zero, i.e., $(x_k+\Delta)\cdot n_0\left[(x_k+\Delta)^2\right]-y=0$;

4) Expand the equation above by Taylor series as $f(x_k)+\left[n_0'(x_k^2)\cdot 2x_k^2+n_0(x_k^2)\right]\cdot\Delta=0$, where n_0' is the derivative of n_0, i.e., $\frac{dn_0(x_k^2)}{d(x_k^2)}$;

5) The correction can be solved from the equation above as $\Delta=-\frac{f(x_k)}{n_0'(x_k^2)\cdot 2x_k^2+n_0(x_k^2)}$;

6) According to the fact n_0 and n_0' are close to 1, the correction can be approximated as $\Delta=-\frac{f(x_k)}{1+2x_k^2}$. Iterate steps 2, 3, 4, 5 and 6 until $|f(x_k)|<\varepsilon_2$, where ε_2 is a small value, e.g.1×10^{-7} used in this paper. Thus, the value of x_k at this iteration is the required zero root.